

## Research Paper

## A united WRF/TRNSYS method for estimating the heating/cooling load for the thousand-meter scale megatall buildings

Junliang Cao <sup>a</sup>, Jing Liu <sup>a,b,\*</sup>, Xiaoxin Man <sup>a,c</sup><sup>a</sup>School of Municipal and Environmental Engineering, Harbin Institute of Technology, Harbin, China<sup>b</sup>State Key Laboratory of Urban Water Resource and Environment, Harbin Institute of Technology, Harbin, China<sup>c</sup>China Construction Engineering Design Group Corporation Limited, Beijing, China

## HIGHLIGHTS

- Vertical weather condition is explored by mesoscale meteorological model WRFv3.4.
- Weather database of TRNSYS16 is corrected in terms of height by the WRF results.
- A method is developed to calculate the heating/cooling load for megatall buildings.
- Effect of room height on heating/cooling load is investigated for megatall buildings.
- Height correction factor of heating/cooling load is defined and analyzed.

## ARTICLE INFO

## Article history:

Received 17 September 2016

Revised 4 November 2016

Accepted 27 November 2016

Available online 28 November 2016

## Keywords:

Thousand-meter scale megatall building

WRF

TRNSYS

Heating/cooling load

Thermal load

## ABOUT

A united WRF/TRNSYS method is developed to calculate the heating/cooling load for the plan of constructing the thousand-meter scale megatall building in this study. The core of the united WRF/TRNSYS method consists of three parts: (1) utilizing mesoscale meteorological model WRFv3.4 (Weather Research & Forecasting Model) to obtain the vertical distribution of atmospheric temperature and wind velocity in a particular region, (2) correcting weather database of TRNSYS16 (Transient Systems Simulation Program) based on results from (1), (3) calculating the heating/cooling load using the corrected weather database for a megatall building. To better illustrate the utilization of the very method, the heating/cooling load is calculated for a hypothetical thousand-meter scale megatall building in the site of Dalian, China. We assumed the building would be used primarily for commercial office purposes. The results show that the building cooling load gradient with height is approximately  $-2$  to  $-2.5 \text{ W m}^{-2} \cdot 100 \text{ m}^{-1}$ , while the heating load gradient with height is approximately  $+1.2$  to  $+2.5 \text{ W m}^{-2} \cdot 100 \text{ m}^{-1}$ . Compared with the heating/cooling load close to the ground, the cooling load of rooms at 1000 ms (m) above the ground decreases by about 25%, while the heating load increases by about 10%, under the design conditions.

© 2016 Elsevier Ltd. All rights reserved.

## 1. Introduction

## 1.1. Background

With the rapid progress of urbanization, together with the development of new, light-weight materials and advanced construction techniques, the tall-buildings boom of the past decades has been unprecedented in that it has occurred across virtually the entire globe, simultaneously.

**Fig. 1** shows that, globally, the total number of existing buildings over 200 ms (m) has more than doubled in the last ten years [1]. According to the Council on Tall Buildings and Urban Habitat (CTBUH), a supertall building is defined as a building taller than 300 m, and a megatall building is defined as a building over 600 m [2]. Burj Khalifa, is presently the tallest building in the world at a height of 828 m. Furthermore, the world's first thousand-meter scale building, Kingdom-Tower, in Jeddah, Saudi Arabia, is set to be constructed in this decade, with a designed building height of 1000 m. This means that the world is expected to enter the era of the thousand-meter scale megatall building in the foreseeable future.

\* Corresponding author at: School of Municipal and Environmental Engineering, Harbin Institute of Technology, Harbin, China.

E-mail address: [liujinghit0@163.com](mailto:liujinghit0@163.com) (J. Liu).

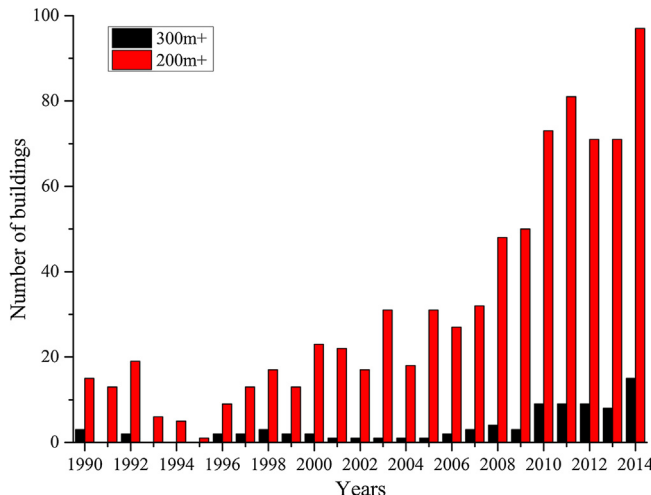


Fig. 1. Number of tall buildings over 200 m and 300 m [1].

Additionally, what is more interesting than the number of buildings and their heights is that the function of the tall buildings has been changing, as shown in Fig. 2. The ratio of residential and mixed-use functions has increased, from 12% at the turn of this century, to 53% currently; office space is still a large proportion of the total use.

With the increase in the number of buildings and their heights, the heating/cooling load calculation for megatall buildings has created new challenges for designers. Conventionally, the evaluation of the heating/cooling load uses values from atmospheric temperatures and wind velocities at the meteorological station level (at approximately 2 m or 10 m above the ground). For example, the Ref. outdoor atmospheric temperature for a heating/cooling load calculation, given by the ASHRAE standard, is a constant for the particular site, and the ASHRAE 'standard' value for the convective heat transfer coefficient (CHTC) at the building's external surface is about 31 W/(m<sup>2</sup> K) at a wind velocity of 6.7 m/s [3]. In past years, standard practice worldwide did not consider the potential variation in this coefficient in the vertical direction. However, it is obvious that this practice is adaptable only for relatively 'low' buildings, namely those where the variation of atmospheric

parameters around the building in the vertical direction is minor enough to be ignorable.

In terms of the megatall buildings, the prominent feature of building height, has gone far beyond most existing buildings, even exceeding the top of the atmospheric boundary layer. The vertical variation of atmospheric temperatures and wind velocities surrounding the building may exhibit noticeable variability, and the corresponding heating/cooling load cannot be predicted accurately if this is not taken into consideration. Incorrect predictions will lead to the decreased comfort of occupants or an increase in building energy consumption.

In recent years, some researches have been carried out on vertical wind environment in urban regions. For example, Liu et al. [4], conducted computational fluid dynamics simulation of the wind flow over an airport terminal building. Draxl et al. [5], conducted a simulation of wind profile in urban region to evaluate the vertical wind shear using weather research and forecasting model. Mattar and Borvarán [6] represented a simulation of wind velocities at 5 specific heights by mesoscale meteorological model near the central coast of Chile to estimate the wind power. Sakakubara and Nakagawa [7] described the vertical temperature profile with light breeze at night in urban and rural area. However, these studies mentioned before concerned much on the drag effect of buildings on the air flow characteristics in building or building cluster scale, which are, in general, conducted based on existing typical wind profiles through wind tunnel test or computational fluid dynamics (CFD) techniques. The typical wind profiles expressed in empirical power law are basically applied within atmospheric boundary layer, tops out between about 250 and 500 m [8]. It is obvious this height is not applicable to thousand-meter scale megatall building.

In fact, only two megatall buildings exist worldwide, there is a lack of research on the vertical variation of atmospheric parameters to inform accurate prediction of heating/cooling load. In light of the potential construction trend for the megatall buildings, it is therefore an imperative to put forward proper methods for heating/cooling load calculations.

Actually, the building heating/cooling load can be divided into two parts: the heat generation from the internal equipment and occupants, and the heat transfer through the external building surfaces. The first part is governed by the building function. The second part is influenced by a number of factors, such as the thermal physical properties of the building envelope, the wind

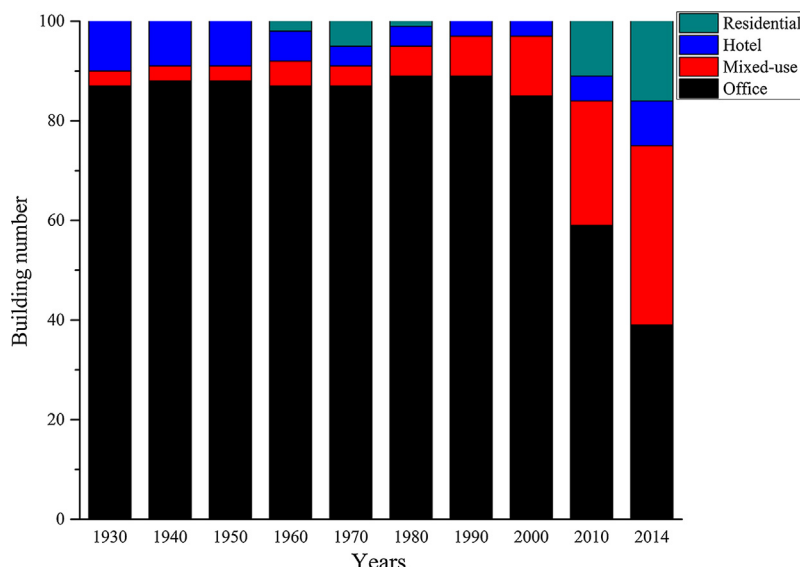


Fig. 2. 100 tallest buildings by function [1].

velocities, and temperature differences between the internal and ambient air. Better understanding of ambient atmospheric parameter distribution can improve the accuracy of heating/cooling load estimations. Currently, conventional method can hardly generate the atmospheric parameters vertical profile covering the megatall building height range, hence, the vertical distribution of heating/cooling load is difficult to calculate accurately.

In this study, we focus on the vertical variation of atmospheric parameters covering the megatall building height range, which represents the meteorological characteristics for urban scale region. A mesoscale meteorological modeling system, therefore, is suggested to simulate regional atmospheric conditions at the urban scale; this information is then linked to a building energy simulation model.

## 1.2. Mesoscale meteorological model

The main mesoscale meteorological models include the Fifth-Generation Pennsylvania State University–NCAR Mesoscale Model (MM5) [9], the Weather Research & Forecasting Model [10], the UK Met Office operational Mesoscale model [11], the French meso-NH model [12], and the NCAR global climate model [13]. They are widely used in regional weather predictions and research. The non-hydrostatic schemes are commonly used in the mesoscale meteorological models, thus the resolution ratio is not suitable for simulating the urban-scale hydromechanics. To solve this problem, the parameterization functions such as the ground surface energy balance function, and drag should be imported into the mesoscale meteorological model; the influence of urban canopy should also be considered. Following research over the last decade in how to appropriately downscale the utilization of mesoscale meteorological models, remarkable progress has been made in introducing these models into urbanization schemes [14]. There has also been significant research looking at the combination of mesoscale meteorological models and computational fluid dynamics (CFD). In these cases, calculation results of the mesoscale meteorological model have always been used as the boundary condition [15].

The Weather Research & Forecasting Model (WRF) is a well-known mesoscale meteorological model, developed for both research and application, and can be used for simulations across spatial scales varying from tens of meters to thousands of kilometers, with a horizontal grid spacing of  $10^1\text{--}10^6\text{ m}$  and a vertical grid spacing grid of  $10^1\text{--}10^3\text{ m}$ . The core equation set for WRF is fully compressible, Eulerian and nonhydrostatic with a run-time hydrostatic option. The model uses terrain-following, hydrostatic-pressure vertical coordinate with the top of the model being a constant pressure surface. The horizontal grid is the Arakawa-C grid. The time integration scheme in the model uses the third-order Runge-Kutta scheme, and the spatial discretization employs 2nd to 6th order schemes. The model supports both idealized and real-data applications with various lateral boundary condition options. The model also supports one-way, two-way and moving nest options.

The terrestrial data sets for the WRF model are built using the National Centers of Environmental Prediction (NCEP) geographical data. These global data sets include soil categories, land-use, terrain height, annual mean deep soil temperature, monthly vegetation fraction, monthly albedo, maximum snow albedo, and slopes. The NCEP final analysis data from the Global Data Assimilation System (GDAS) was used to supply the initial and boundary conditions, which continuously collects observed data from the Global Telecommunications System (GTS), and other sources, including surface pressure, sea level pressure, wind velocity, wind direction, temperature, sea surface temperature etc. Also the model has a number of options for various physical processes. For example, the cloud microphysics schemes are used to model the microphysical processes that govern cloud particle formation,

growth, and dissipation on a small scale [16]. The effect of sub-grid-scale clouds are represented by cumulus parameterization schemes. The short and long wave radiation schemes provide the atmospheric heating profiles, and allow estimation of net radiation for the ground heat budget. The surface layer (SL) schemes are used to calculate the friction velocity, and exchange coefficients that enable the estimation of heat, momentum, and moisture fluxes by the land surface models (LSM). The planetary boundary layer (PBL) schemes determine the flux profiles within the convective boundary layer, the stable layer, and thus provide atmospheric tendencies of temperature, moisture and momentum in the entire atmospheric column.

In the last decade, a lot of researches have been carried out to examine the accuracy of WRF model, and the validity has been verified on the time scale of hours. Shrivastava et al. [17] analyzed various combination of parameterization schemes in predicting surface and upper meteorology around the Kaiga nuclear power plant site by comparing predicted data with measured data. Borge et al. [18] performed an extensive sensitivity analysis of meteorological input parameters for atmospheric temperature over the Iberian Peninsula. Carvalho et al. [19] assessed the sensitivity of 5 different planetary boundary layer parameterization schemes of wind simulation, and the results were compared to the measured wind data collected at coastal areas, which aims to estimate the wind energy production. The studies above show that no major differences between the predicted data and measured data are seen among the simulations, such as wind velocity, wind direction and air temperature.

It should be noted that WRF model, in essence, is a forecasting tool by incorporating various information simulated from 'historic' observed data on the mesoscale grid. The observed data includes direct observations from surface and radiosonde reports and indirect observations remote sensing techniques, and objective analysis for future information are conducted to realize the forecast function [20]. However, in present study, only the data during the 'historic' observation period in the result file is concerned to ensure the validity, based on which atmospheric parameter vertical profile in the objective domain can be established by interpolating.

## 1.3. Building energy simulation program

Building energy simulation programs are increasingly used to analyze the energy performance of buildings, and the thermal comfort of occupants [21]. Generally, building energy programs can be divided into the following two categories:

- (1) Models that focus on the working processes of the energy system components. Representatives of this category include HVACSIM+ [22], and SPARK [23]. These models consist of relatively simple building models and complex component models; the system is flexible and can be set up according to the user's needs. These models are open source; users can not only improve the models, but also define a new model based on an actual component.
- (2) Models that focus on the dynamic simulation of the building energy consumption. Representatives of this category are EnergyPlus, and DeST [24,25]. These simulation programs are made up of a functional building model and a simplified energy system model. They are suitable for the long-term dynamic simulations of the building.

The energy simulation software TRNSYS 16 is a modular program package that was developed for transient energy system simulations [26]. It consists of two parts. The first part is an engine that reads and processes the input file, iteratively solving the system, determining convergence, and plotting the system variables. The second part is

an extensive library of components, each of which models the performance of one part of the system. The standard library includes a variety of models such as multi-zone buildings, weather data processors, economics routines, and basic air-conditioning equipment. In this research, TRNSYS 16 was selected as the building energy simulation tool of choice due to the modular nature of the simulation software, and well-documented programming interface. It is also possible to extend TRNSYS 16 with self-developed modules. With the aid of TRNSYS Studio, a user can easily build a complex simulation program, which consists of different "Types" connected to each other. To date, a considerable amount of research has been carried out to model new or unconventional systems by developing new modules with TRNSYS [27]. TRNSYS is capable of accepting many forms of weather data. Among them, the TMY (typical meteorological year) database is most widely used.

The aim of this study is to develop a united WRF-TRNSYS method able to calculate the dynamic energy consumption of a thousand-meter scale megatall building under specific meteorological conditions. Use of this method is illustrated by simulating a hypothetical, megatall building in the city of Dalian, China.

In the next section, we describe the calculating procedure of the united WRF/TRNSYS method. Section 3 gives an example of applying the united WRF/TRNSYS method to calculate the vertical profile of atmospheric parameter and the vertical distribution of heating/cooling load in a hypothetical thousand-meter megatall building in the site of Dalian, China, and some conclusions are summarized in Section 4.

## 2. Methodology

### 2.1. Calculation flowchart of the united WRF/TRNSYS method

As shown in Fig. 3, the calculation flowchart of the united WRF/TRNSYS method is described below:

Step 1: The meteorological simulation of a particular site is carried out using the mesoscale meteorological model WRF v3.4. The purpose of this step is to provide the vertical profile of atmospheric temperature and wind velocity for Step 2.

Step 2: The weather database of TRNSYS 16 is corrected based on the correlations of the high level data, which is described as the functions of ground surface data and height fitted from the WRF results of Step 1. In the correction, the weather database of TRNSYS16 is regarded as the ground surface data in the function. It should be noted that the WRF model is, in essence, a weather forecasting model. Therefore, this study clearly focused on the variation trends of atmospheric parameters in the vertical direction, through the use of the limited meteorology data for a certain period; it was not based on the statistical data from long-term meteorological observations such as the TMY data used in TRNSYS 16. This important difference separates this work from a conventional simulation of building energy consumption. Additionally, with respect to the CHTC of building external surface, it is corrected according to the correlation of wind velocities at different heights derived from the WRF results.

Step 3: The cooling and heating load of the megatall building at its specific site is calculated by TRNSYS 16, according to the modified climate database established in Step 2.

### 2.2. Calculation conditions

#### 2.2.1. Research site

Dalian is a large city situated on the southern tip of the Liaodong Peninsula; three sides are surrounded by the Bohai Sea. In this region, the Qianshan Mountains and Changbai Mountains,

with an average height of 1200 m, are covered by semi-evergreen forests. Only a small fraction of land is used for agriculture. With respect to weather, Dalian is located in the cold region defined by the *Thermal code for civil building (GB50176-93)*, which has a warm, temperate, continental monsoon climate, with an average annual temperature of 10.5 °C. The predominant wind directions are South East (SE), North East (NE), East (E) and North (N), with the average wind velocity being on the order of 4.5 m/s. This region receives abundant rainfall from January to December, with the cumulative value of about 900 mm.

#### 2.2.2. Calculation conditions for WRF

In our study, the WRF model was designed as follows: the simulation area was made of a quadruply nested grid, with horizontal grid spacing of 81 km, 27 km, 9 km, and 3 km, and 27 vertical levels. Specially, it is set densely for the vertical levels close to ground surface to catch the physical characteristics of the air around the megatall building; the model eta levels, specifically, are 1.000, 0.998, 0.987, 0.976, 0.957, 0.942, 0.899, 0.870, 0.857, 0.726, 0.701, 0.644, 0.576, 0.507, 0.444, 0.380, 0.324, 0.273, 0.228, 0.188, 0.152, 0.121, 0.093, 0.069, 0.048, 0.029, 0.014 and 0.000, which covers east China, centered at the site of Dalian (a point with the coordinates Latitude = 39°54'20", Longitude = 123°25'29"), as shown in Fig. 4. The height of the first five layers in the meteorological data from WRF is approximately 2 m, 28 m, 87 m, 122 m and 198 m. The terrain and land-use data for the innermost domain, with 3 km grid resolution, are taken from 30" data, 5' data are used for the domain with 9 km resolution, and 10' data are used for the domain with 27 km resolution. The model was set up using a single-moment, 6-class microphysics scheme (WSM6), containing ice, snow, and graupel processes, vapor, and rain, the Noah land surface model scheme [28], the PBL scheme, the Yonsei University (YSU) scheme [29], and the RRTM (Rapid Radiation Transfer Model) scheme for radiation [30]. In this study, the whole year of 2012 were selected as the simulation period to explore the vertical atmospheric meteorology characteristic for Dalian site. The time interval of WRF model was set as 2 h for output.

#### 2.2.3. Building model for TRNSYS simulation

As mentioned previously, in Step 2 a new 'Correcter' module was developed to correct the weather data from the 'Weather data' processor module, and then link the corrected data to the multi-zone 'building model' module. The interface of the TRNSYS project with the corrected weather data is shown in Fig. 5.

Because the megatall building for this study is hypothetical, a simple, typical rectangular floor plan of 1000 m high building was proposed to calculate the heating/cooling load, with a floor area of 14,400 m<sup>2</sup>. The aspect ratio of the building was then set at 8.5, which satisfies the requirements of the structure design of super-tall buildings [31]. To simplify the plane layout of the building model, a core tube (elevator hall included) was set at the center of the building plane and the area was set as 2880 m<sup>2</sup>. As office function is still a large proportion of the use case in tall buildings (see Fig. 2), the rest of the area around the core tube was included in the design as office rooms. Each room had an area of 70 m<sup>2</sup> (see Fig. 6). The average story height was set as 5 m.

The calculation conditions of heating/cooling load are shown in Table 1. The office hours are set from 8:00–18:00. According to studies [32], buildings over 500 m must be constructed using a glazing curtain wall for structural safety, therefore the double glazing curtain wall without shading design was selected for this hypothetical megatall building as shown in Table 2, and infiltration was considered to be negligible due to the airtight properties of the glass curtain wall. The thermal physical parameters of building envelope and other calculation conditions were set according to *Design code for heating ventilation and air conditioning of civil build-*

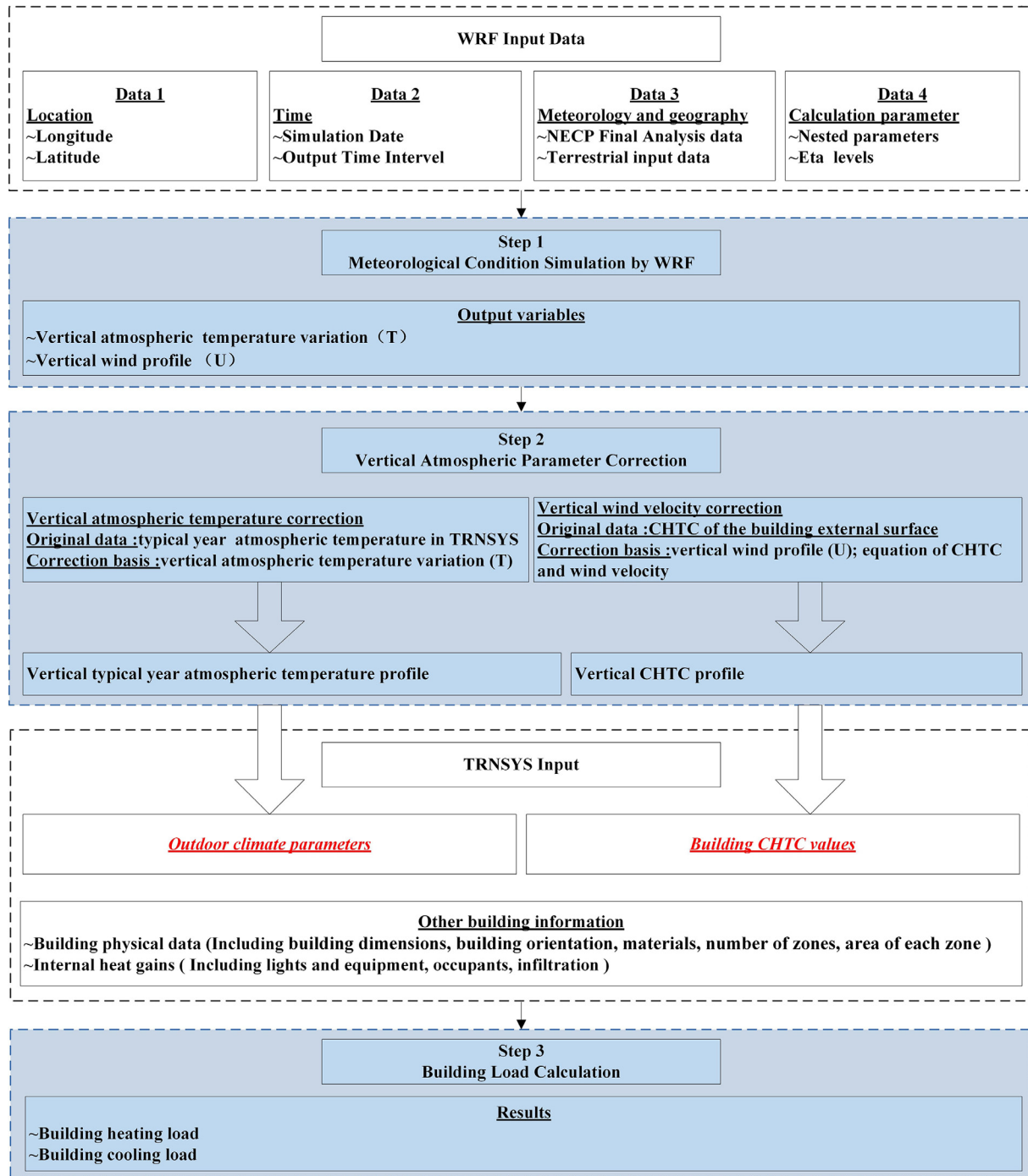


**Fig. 3.** Calculation flowchart of the united WRF/TRNSYS method.

ings (GB 50736-2012). The thermal parameters of main internal structures are summarized in Table 3. To simplify the calculation process, the variation of heat emissions from the equipment and occupants during the office hours, together with setbacks, was not taken into consideration in this study.

### 3. Results and analysis

#### 3.1. Evaluation of the united WRF/TRNSYS method

The united WRF/TRNSYS method is developed to calculate the heating/cooling load for thousand-meter scale megatall building, and the application is discussed as follows:

- (1) It should be noted that only the heat/cooling load can be calculated by the method, which is different from air-conditioning load. As we all know, the air-conditioning load are mainly comprised of three parts: heating/cooling load, fresh air load and other load (reheat load, heat losses from duct, heat losses from equipment). With respect to the vertical variation of fresh air load, it is not considered for the complexity of outdoor enthalpy vertical distribution in the WRF/TRNSYS method at present stage.
- (2) Compared with the conventional building energy simulation program, the united WRF/TRNSYS method, in essence, has taken the vertical variation of atmospheric parameter into consideration, including atmospheric temperature and wind

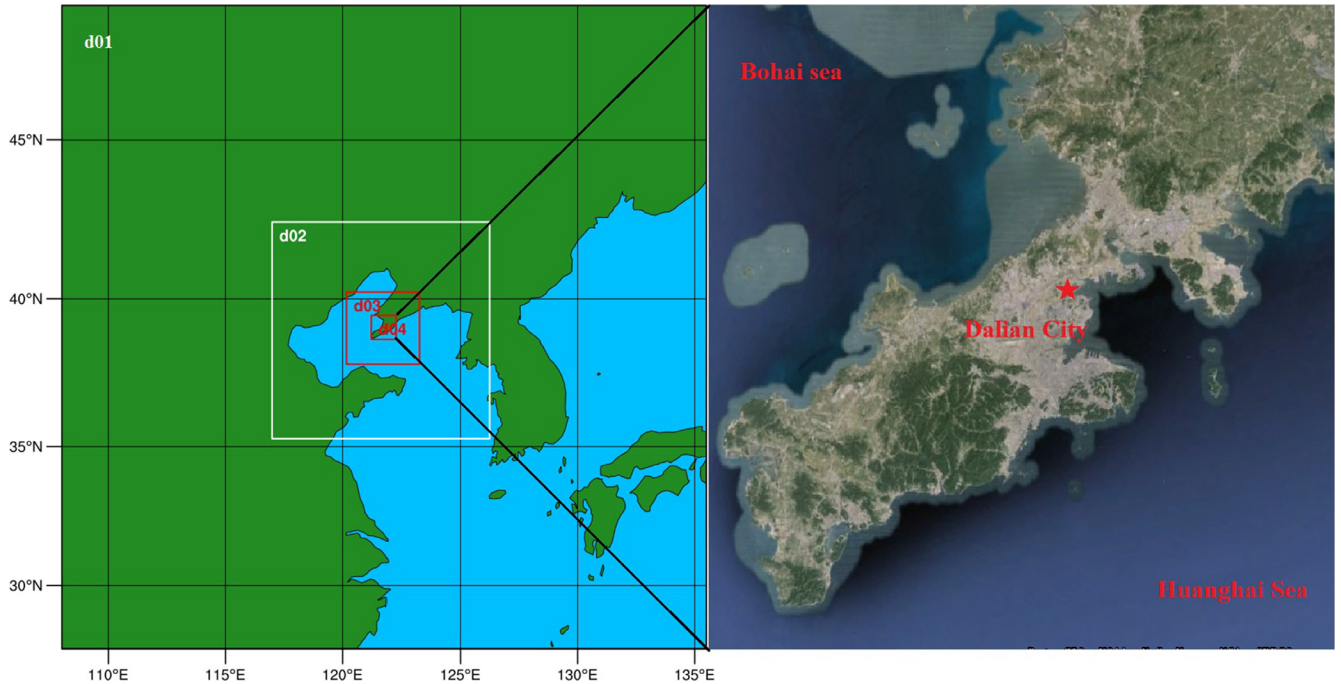


**Fig. 4.** Model domains and the topography of the inner domain (star denotes the location of the building).

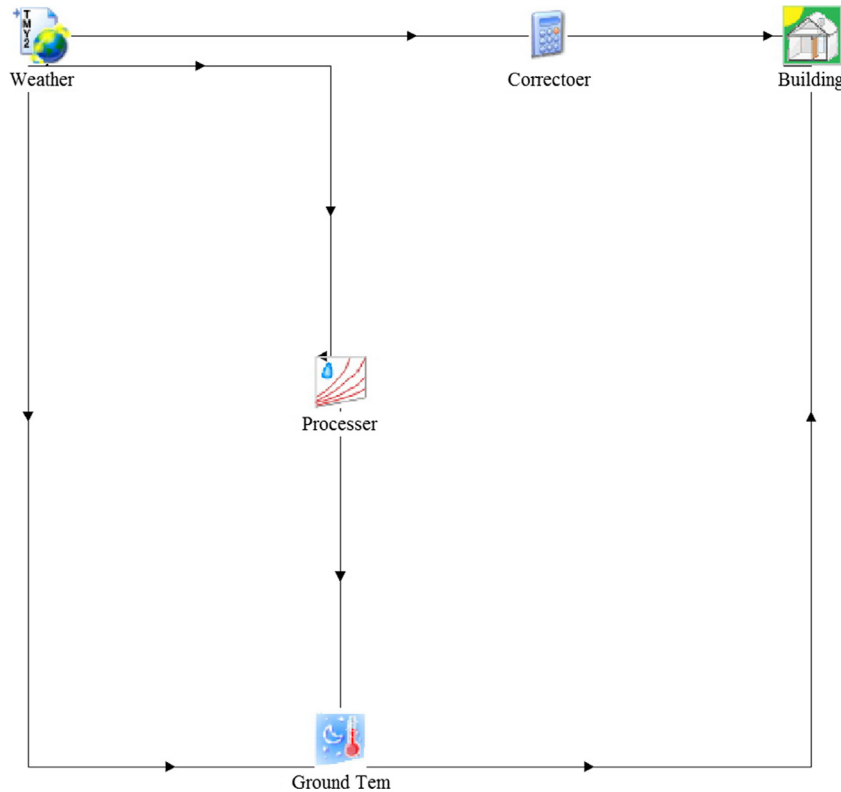


**Fig. 5.** TRNSYS model with the corrected weather data for heating/cooling load calculation.

velocity. In fact, the heating/cooling is influenced by many meteorology factors, such as solar radiation, atmospheric transparency, weather conditions etc. But it is difficult for the researchers to analyze effects of these factors quantitatively. Take the solar radiation for example. Firstly, solar radiation, in theory, is a function of meso-meteorology

however can vary locally through changes in surface albedo, pollution levels and altitude [33]. In cities solar radiation levels are reduced mainly due to polluted urban atmosphere, however, this is typically counteracted by reduced surface albedo leading to only minor variations of the solar radiations experienced along the vertical direction [34]. Secondly,

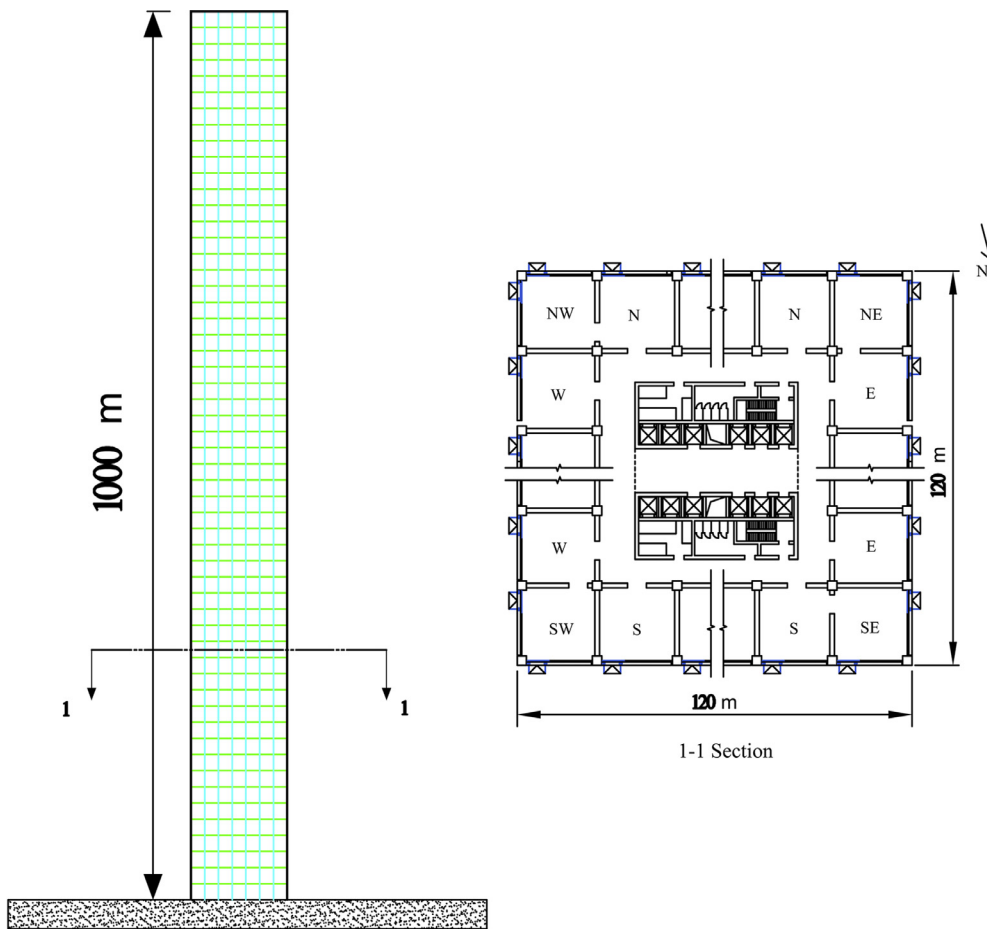


**Fig. 6.** Hypothetical building model for heating/cooling load calculation.

**Table 1**  
Parameters of the heating/cooling load calculations.

Parameters	Values
Indoor set-point temperature for cooling	25 °C
Indoor set-point relative humidity for cooling	60%
Indoor set-point temperature for heating	22 °C
Indoor set-point relative humidity for heating	55%
Lighting and equipment	40 W/m <sup>2</sup>
Occupant activity	Light (12 W/m <sup>2</sup> )

**Table 2**  
The physical parameters of glazing curtain wall.

Property	Value
Types of glazing	
U-value of glazing (W/m <sup>2</sup> K)	2.10
Solar heat gain coefficient	0.19
Visible transmittance	0.71
Coating	Double low-e
Infilling gas	Air
Frame ratio	9.6%
U-value of frame (W/m <sup>2</sup> K)	0.81
U-value of spandrel (W/m <sup>2</sup> K)	0.22

for buildings, the areas of a megatall building above the urban canopy layer, with greater exposure and reflections from adjacent rooftops, will typically receive greater solar radiation than below the urban canopy which may be shaded for portions [35]. Because the megatall building in this paper is hypothetical, we can disregard the effect of

adjacent buildings. Finally, the vertical distribution of solar radiation is influenced by weather condition, aerosol effect as well. It would make the simulation process much complex in WRF model if the solar radiation variation is taken into consideration in urban scale. Overall, with the reasons above, vertical variation of some complex factors are ignored in the united WRF/TRNSYS method.

(3) Additionally, the vertical profiles in this paper is simulated from mesoscale meteorological model, and that means the specific surroundings, such as buildings, microscale artificial environment, is out of consideration, which would influence the building-scale environment. Actually, just as the database in the building codes for heating/cooling calculation, the vertical profiles are established to represent the atmospheric distribution characteristics in urban scale. With regard to the effect of specific surroundings, it can be corrected by the designers according to the actual conditions.

### 3.2. Validation of WRF model

To validate the performance of WRF model in reproducing the vertical atmospheric parameters, comparisons are made between the WRF results and radiosonde data obtained from China Meteorological Administration at Dalian observatory (<http://data.cma.cn/data/detail/dataCode/B.0011.0001.C.html>). The radiosonde data for validation was observed on January 6th and July 7th in 2012, because these days were considered as clear weather, during which the data integrity and reliability can be guaranteed. The data are linearly interpolated for comparison with the WRF results in

**Table 3**

Material layers of main internal structures.

Internal structures	Layer	Thickness (mm)	Conductivity (W/m K)	Density (kg/m <sup>3</sup> )	Specific heat (J/kg K)
Internal floor	Lime mortar	30	0.79	1600	1050
	Insulation	20	0.08	400	1057.7
	Reinforced concrete	120	1.72	2500	920
	Lime mortar	30	0.79	1600	1050
Internal wall	Lime mortar	30	0.79	1600	1050
	Reinforced concrete	120	1.72	2500	920
	Lime mortar	30	0.79	1600	1050

the vertical direction. Therefore, two WRF simulations are conducted for the comparison in total, and each simulation is for 3 day period, one on the day of the observation occurrence, 1 day prior and 1 day later to it for the model stability [17]. It should be noted that the radiosonde sounding is carried out twice a day (6:00 and 18:00), hence a 2 day radiosonde data provides 4 datasets for comparison in the verification.

Fig. 7 shows the comparisons between the WRF results and radiosonde data corresponding to the observation time in the vertical direction from 0 to 1000 m. Overall, it can be seen the observed atmospheric temperature and wind profiles are well reproduced by the WRF model. For the atmospheric temperature, it is seen that the WRF results are a little larger, approximately 0.5 °C, than the radiosonde data. It can be attributed to the deficiency of the horizontal resolution of the mesoscale meteorological model in capturing the atmospheric parameter at one point, for which the atmospheric parameters at any point in the gridding area are represented by the area mean value [20]. On the other hand, the vertical variation trend observed by the radiosonde are well reproduced by WRF model. Therefore, it can be concluded that

WRF model is applicable for exploring the vertical variation regularity of atmospheric parameters up to 1000 m.

### 3.3. Vertical profile of atmospheric parameters of Dalian site

According to the long-term investigation on local meteorology, January and July are representative of the meteorological characteristics of winter and summer in Dalian, respectively [36]. The results of the atmospheric parameters in these two months derived from the innermost domain, at 3 km resolution covering the Dalian site, are presented as typical months to describe the vertical atmospheric distribution characteristic in Dalian site below. We defined the monthly averaged values of the central point as the indicators of local meteorology for the innermost domain.

#### 3.3.1. Vertical profile of atmospheric temperatures

The vertical profiles of the monthly mean atmospheric temperature in January and July are shown in Fig. 8. It is found that the temperature decreases in an approximately linear curve as the height increases, with a gradient of approximately

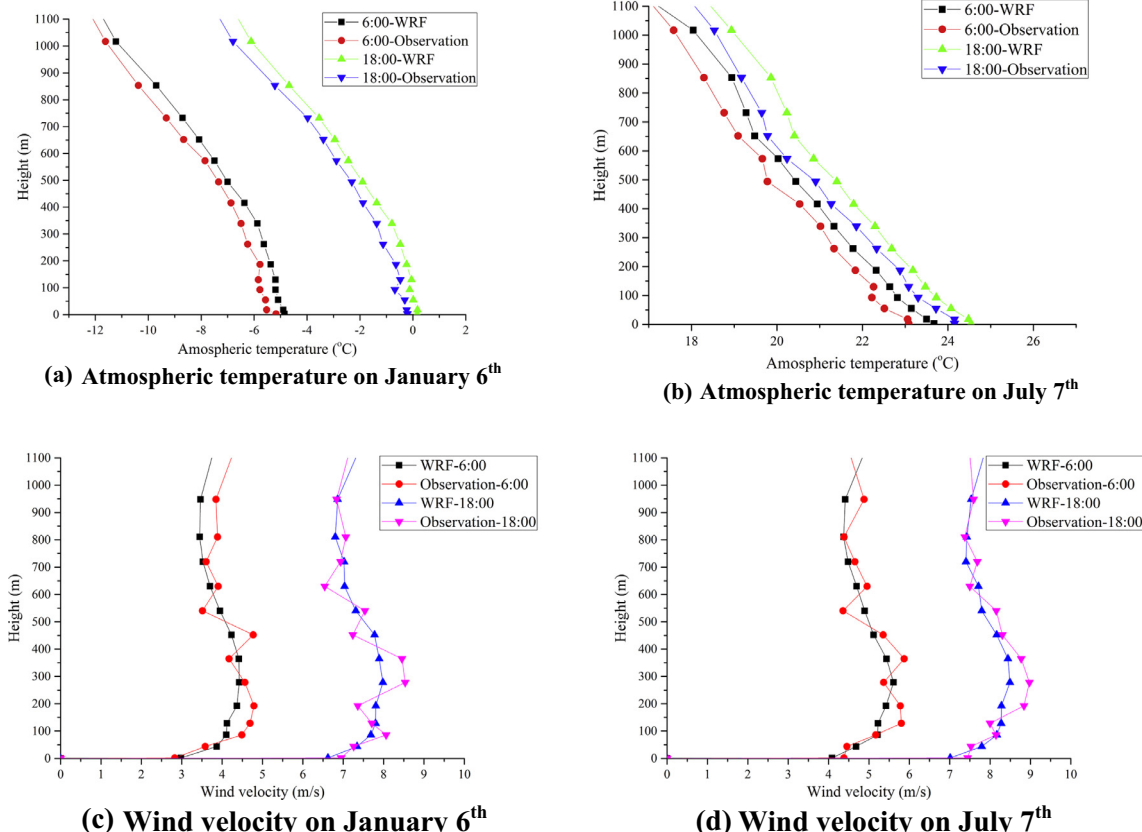


**Fig. 7.** Comparisons between the WRF results and radiosonde data. (a) Atmospheric temperature on January 6th, (b) Atmospheric temperature on July 7th, (c) Wind velocity on January 6th, (d) Wind velocity on July 7th.

$-0.58^{\circ}\text{C}/100\text{ m}$  of height, which is independent of the season. Additionally, the daily variation of monthly mean temperatures at heights close to the ground (0 m in the figure), 300 m, 500 m, 800 m, and 1000 m above the ground is calculated and plotted in Fig. 9. This shows that the variations of atmospheric temperatures at different times are, on the whole, similar to each other. They gradually rise from the minimum value observed at 2:00 at night, and reach a peak value around 14:00 the afternoon. Additionally, it should be noted that the atmospheric temperature difference at different heights is not the same throughout the day, or during different seasons. For example, in summer at 14:00, the atmospheric temperature close to the ground is about  $31^{\circ}\text{C}$  and the atmospheric temperature at a height of 1000 m is about  $18^{\circ}\text{C}$ . However, the atmospheric temperature difference is only about  $5^{\circ}\text{C}$  at 2:00. Compared to the summer, the atmospheric temperature difference is relatively small during the winter. This may be due to the interaction of solar radiation and ground reflection, which would affect the atmospheric temperature close to the ground significantly, and then affect the corresponding vertical profile to a lesser degree.

The atmospheric temperature variations with time and height, in January and July, are fitted respectively as below:

$$\theta_1(t, h) = -4.15 - 2.14 \cos(0.2652t) - 4.8 \sin(0.2652t) - 0.0057h \quad (R^2 = 0.92) \quad (1)$$

$$\theta_7(t, h) = 25.12 - 4.29 \cos(0.2652t) - 2.469 \sin(0.2652t) - 0.0058h \quad (R^2 = 0.93) \quad (2)$$

where  $\theta_1(t, h)$  and  $\theta_7(t, h)$  are the atmospheric temperatures in January and July ( $^{\circ}\text{C}$ ),  $t$  is time in one day, and  $h$  is the height above the ground.

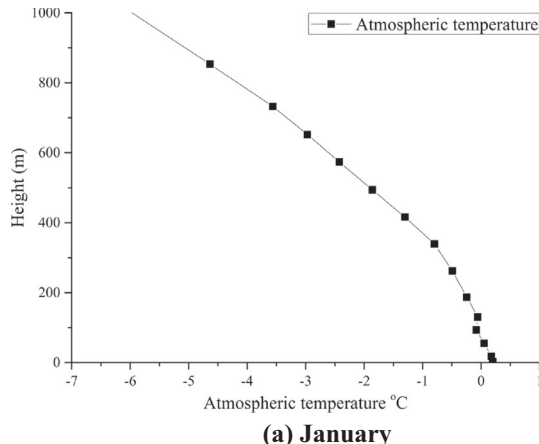
The mean atmospheric temperature of different heights in the vertical direction can also be fitted based on the reference temperature which is close to the ground:

$$T_1(h) = T_b - 0.0057h - 0.3149 \quad (R^2 = 0.95) \quad (3)$$

$$T_7(h) = T_b - 0.0058h - 0.3837 \quad (R^2 = 0.96) \quad (4)$$

where  $T_1(h)$  and  $T_7(h)$  are the atmospheric temperatures in January and July ( $^{\circ}\text{C}$ ), and  $T_b$  is the atmospheric temperature close to the ground.

Corresponding to Step 2 of the united method, the atmospheric temperature module for correction is developed based on Eqs. (3) and (4), which link the weather data module and building model module in Fig. 5, here  $T_b$  is typical meteorological year atmospheric temperature from the weather database of TRNSYS16.



(a) January

### 3.3.2. Vertical profile of atmospheric wind velocities

The vertical profiles of the monthly mean wind velocities in January and July are calculated and plotted in Fig. 10. The figure shows that, although a difference exists between the wind profiles for these two months, the pattern of the profiles is relatively similar. The vertical variation of wind velocity with the height is relatively complex, as compared to that of atmospheric temperature. It can be seen that the wind profile appears exponential at heights ranging from 0 m to approximately 300 m above the ground, with the wind velocities reaching a maximum value (4.6 m/s in January, and 6.7 m/s in July), at the height of 300 m. At heights of 300–800 m, the wind velocity decreases gradually with the increase in height. Above 800 m, the wind velocity increases slightly with height up to the top of the building.

With regard to the CHTC, we refer to the correlation between CHTC and the wind velocity proposed by ASHRAE standard [3]:

$$\alpha_w = 3.8 v_s + 5.7 \quad (5)$$

where  $\alpha_w$  is the CHTC ( $\text{W/m}^2 \text{K}$ ), and  $v_s$  is the local wind velocity at different heights (m/s).

The CHTC vertical profiles at the external surface are then calculated, based on the mean wind velocity profile derived from the results of January and July, as shown in Fig. 11. It can be seen that the trend in variation of CHTC values in January is generally similar to that in July. Taking July as example, the CHTC gradually increases and reaches a peak value at the height of 300 m, of about  $31 \text{ W/m}^2 \text{K}$ , which is as large as the estimated value according to the ASHRAE standard. In fact, except at the height of 300 m above the ground, the CHTCs at most heights are smaller than the estimated value according to the ASHRAE standard.

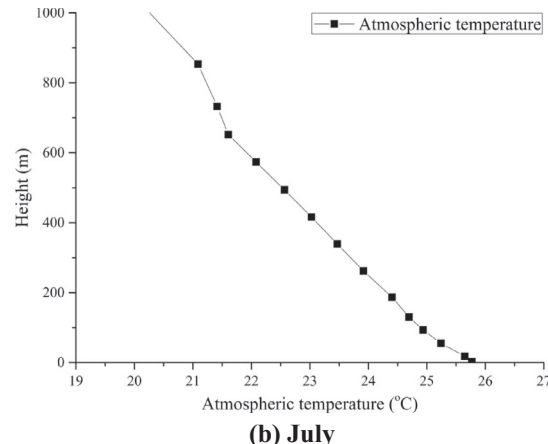
As mentioned before, the CHTC of the external surface at different heights in the building model module is set according to the value in Fig. 11.

### 3.4. Vertical distribution of building cooling and heating load

Based on the vertical variation regularity of atmospheric parameters obtained from the typical months, the cooling/heating load related parameters in TRNSYS model are corrected, and thereby we calculate the building cooling and heating load in the typical months for the hypothetical thousand-meter scale megatall building.

#### 3.4.1. Cooling load calculation and analysis

The daily variations of mean hourly cooling loads at the height of 0 m, 300 m, 500 m, 800 m, and 1000 m above the ground are calculated by TRNSYS. The hourly cooling load simulation is launched



(b) July

Fig. 8. Monthly mean atmospheric temperature vertical profiles. (a) January, (b) July.

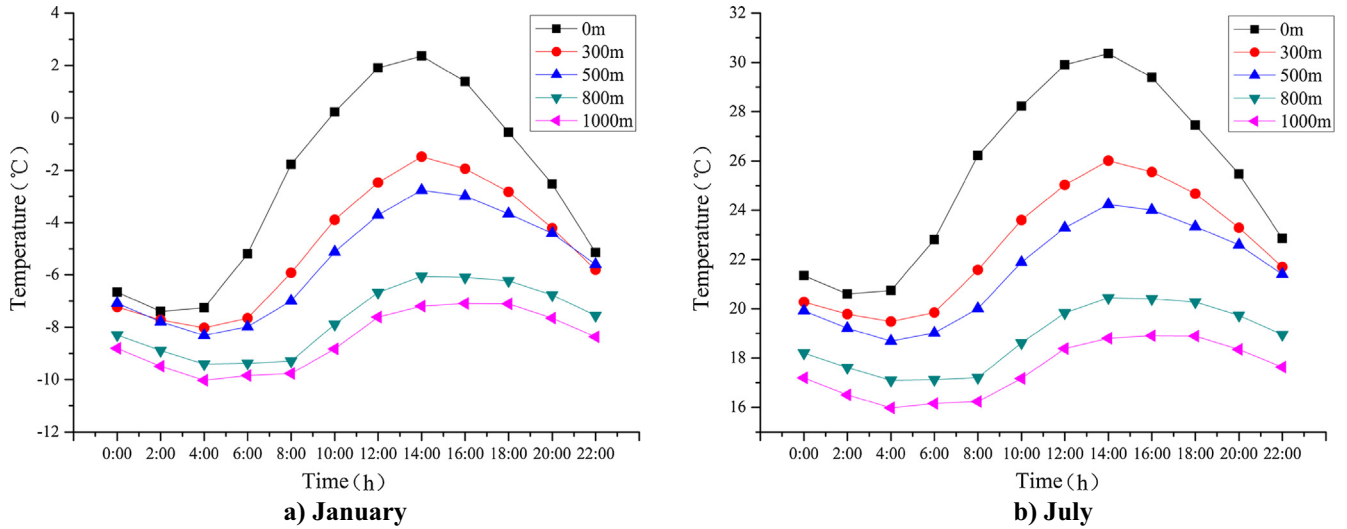


Fig. 9. Daily variation of monthly mean temperatures. (a) January, (b) July.

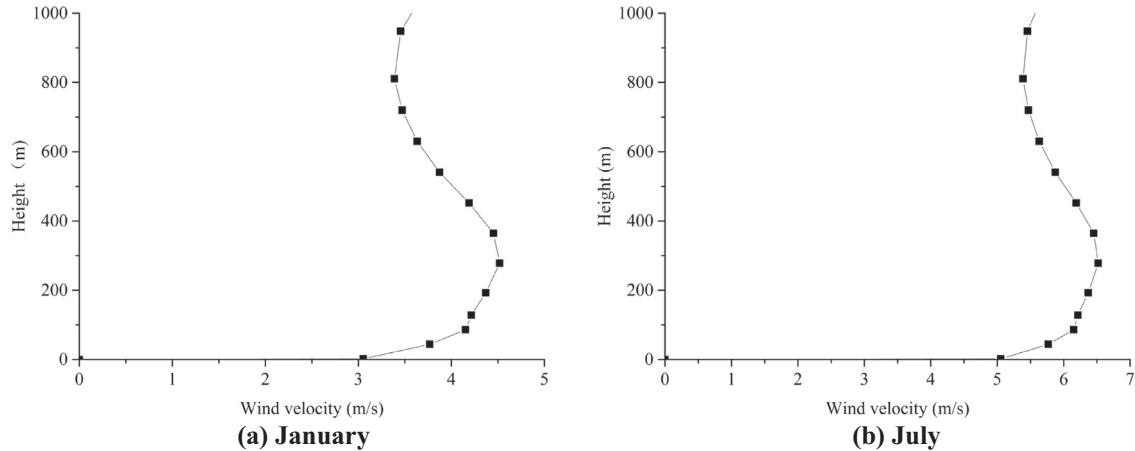


Fig. 10. Monthly mean wind velocity profiles. (a) January, (b) July.

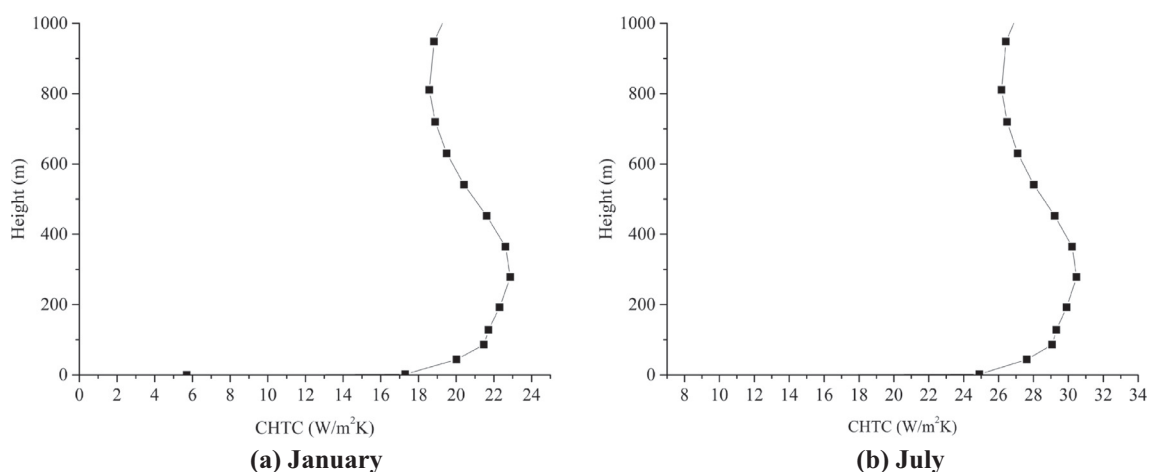
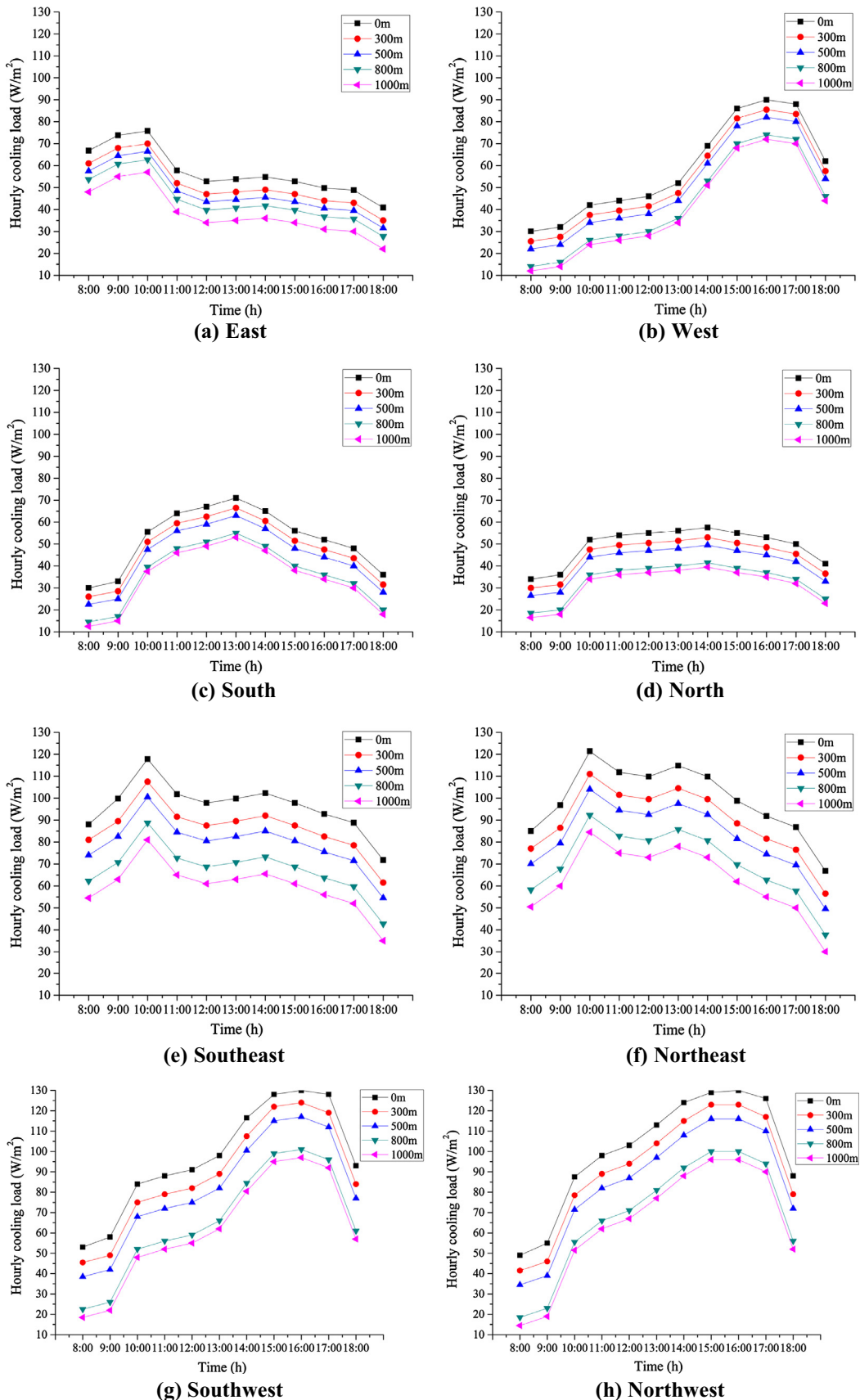


Fig. 11. CHTC vertical profiles at the building external surface. (a) January, (b) July.



**Fig. 12.** Daily variation of cooling load of rooms with different heights and orientations. (a) East, (b) West, (c) South, (d) North, (e) Southeast, (f) Northeast, (g) Southwest, (h) Northwest.

one week prior to July 1st to eliminate the effects of the initial condition. As shown in Fig. 6, different amounts of solar radiation enter the rooms with different orientations, and some have different numbers of external walls; therefore, the corresponding hourly cooling load will be different. The hourly cooling load of a room is plotted with different orientations in Fig. 12.

It should be noted that for the rooms with different orientations, the vertical variation trend of the hourly cooling load is similar; the hourly cooling load decreases with the increase of the height. The main reason is due to the decrease in atmospheric temperature with height in July (see Fig. 8). For rooms with one external glass curtain wall, the building hourly cooling load gradient with height is about  $-2 \text{ W}\cdot\text{m}^{-2}\cdot100 \text{ m}^{-1}$ . For a room with two external glass curtain walls, the building hourly cooling load gradient with height is approximately  $-2.5 \text{ W}\cdot\text{m}^{-2}\cdot100 \text{ m}^{-1}$ . Additionally, it is clear that the hourly cooling loads in the rooms with two external walls are larger than in the rooms with only one external wall. Comparing the hourly cooling loads between the

rooms of west, southwest and northwest, the maximum value appears at approximately the same time, 16:00. However, the hourly cooling load of southwest and northwest orientation is 1.44 times larger than the western orientation. It is seen that the peak values of hourly cooling loads vary with time and orientation; this is consistent with the time of maximum solar radiation. For the rooms oriented to the east, west, south and north, the peak value of hourly cooling load appears at approximately 10:00, 16:00, 13:00 and 14:00, respectively; the room with northern orientation has the overall minimum peak load.

### 3.4.2. Heating load calculation and analysis

As the indoor-outdoor temperature difference is relatively large, the hourly heating load has smaller fluctuations; therefore, the heating load is defined as the maximum hourly heating load during the calculation period of this study, namely the lowest outdoor temperatures at different heights during January. The heating load of the room with different orientations is plotted in Fig. 13. As the

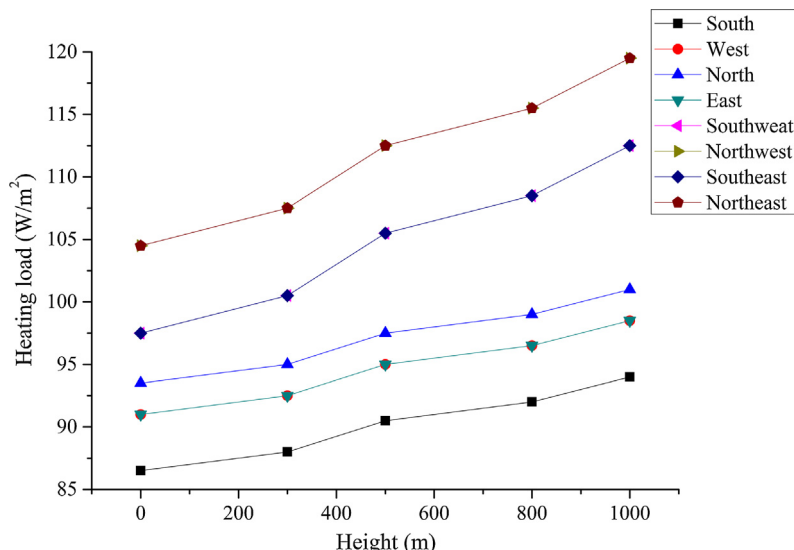


Fig. 13. Heating loads of room with different heights and orientations.

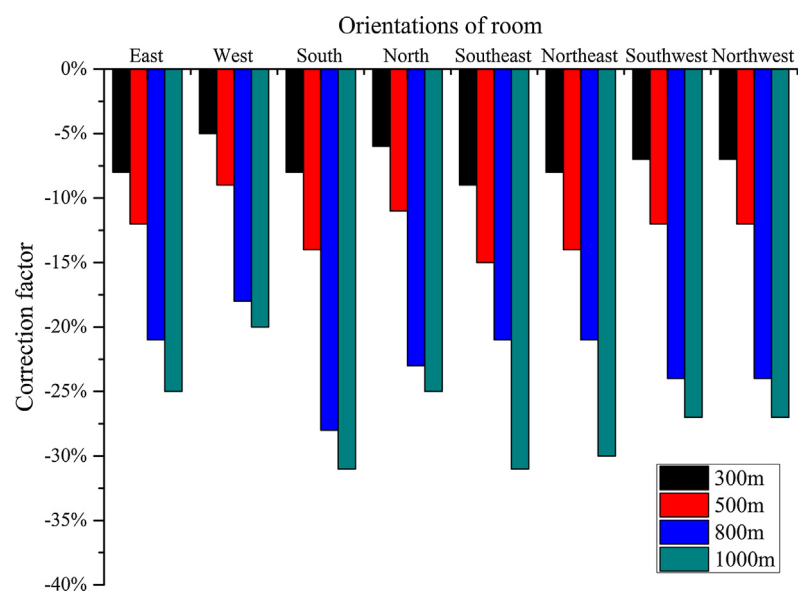


Fig. 14. Cooling load correction factors at different heights.

effect of orientation on the rooms in the east and west is the same, in this case, the heating load for these two orientations is the same. The heating loads for rooms of southeast and southwest orientation show similar results.

The atmospheric temperature decreases with height during the winter; therefore, the heating load increases with the approximately linear increase in height, regardless of orientation. In terms of the heating load for a room with only one external glass curtain wall, the heating load gradient of height is about  $+1.2 \text{ W}\cdot\text{m}^{-2}\cdot100 \text{ m}^{-1}$ , and the room with southern orientation has the minimum heating load. The heating load gradient with height is about  $+2.5 \text{ W}\cdot\text{m}^{-2}\cdot100 \text{ m}^{-1}$  for the room that has two external glass curtain walls. As might be expected, the heating loads of the rooms with two external walls are larger than the rooms with only one external wall. In addition, it is found that the relationship between heating load and the height is not simply linear. For example, close to the ground, the southeast orientation shows a heating load gradient of approximately  $+2.1 \text{ W}\cdot\text{m}^{-2}\cdot100 \text{ m}^{-1}$ , while the gradient at the height of 1000 m is approximately  $+2.5 \text{ W}\cdot\text{m}^{-2}\cdot100 \text{ m}^{-1}$ .

### 3.4.3. Correction factor for building cooling/heating load

To evaluate the variation trend with height identified in this study, the correction factor at different heights for the building cooling or heating load is defined as follows:

$$C = \frac{Q_0 - Q_h}{Q_0} \times 100\% \quad (6)$$

where  $C$  is the heating/cooling load correction factor,  $Q_0$  is the heating/cooling load for a room close to the ground, and  $Q_h$  is the heating/cooling load of a room at the height of  $h$  above the ground. For the parameter in the definition of  $C$ , both the cooling load and the heating load are defined as the maximum hourly value of load during the calculation period.

The cooling and heating load correction factors are shown in Figs. 14 and 15, respectively. It is seen that the cooling load correction factors at different heights are all negative, and the heating load correction factors at different heights are all positive. But overall, the absolute values increase with the height. The cooling load factors range from  $-25\%$  to  $-35\%$  for the rooms of different

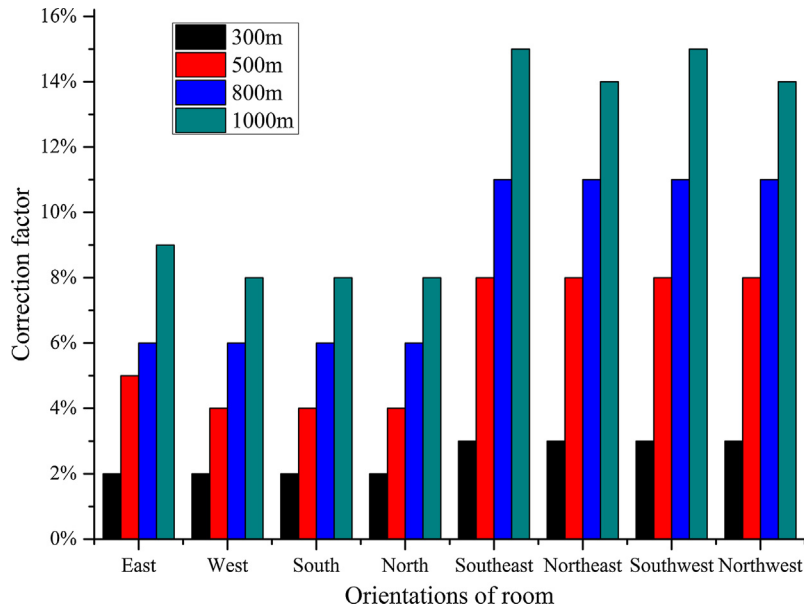


**Fig. 15.** Heating load correction factors at different heights.

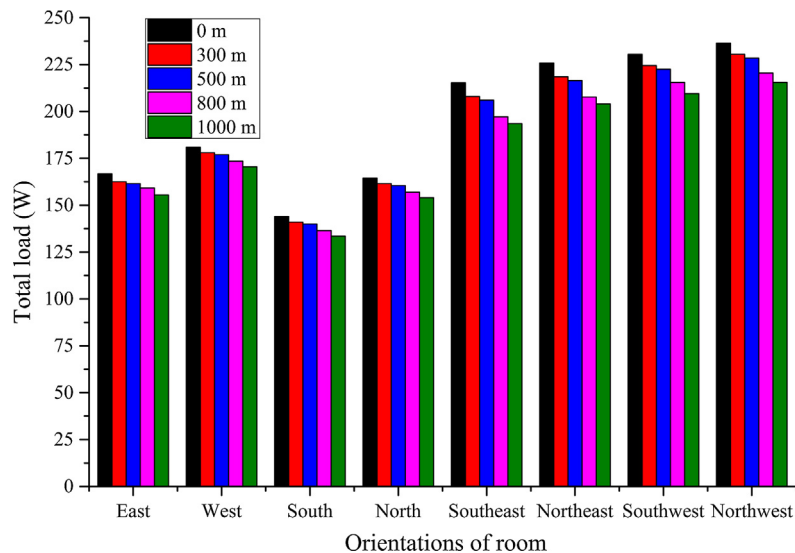


**Fig. 16.** Total loads of room with different heights and orientations.

orientations at the height of 1000 m. Clearly observable is the difference in the cooling load correction factor for the rooms of different orientations. For rooms with one external glass certain wall, the room with southern orientation has the maximum correction factor, the mean correction factor of 300 m, 500 m, 800 m and 1000 m is 0.8%/100 m, 1.3%/100 m, 2.8%/100 m, and 3.2%/100 m, followed by east, north and west orientation, respectively.

The heating load factors range from +8% to +15% for the rooms of different orientations at the height of 1000 m. Compared with the cooling load correction factor, as the heating load variation value of  $Q_o - Q_h$  is relatively small, the values of the heating load correction factors are much smaller than those of the cooling load. On the other hand, it should be noted that the difference between the room orientations is more remarkable, and the rooms with two external glass certain wall have a larger correction factor than the rooms with one external glass curtain wall. This is mainly because the heat transferred from the external wall plays an important part in influencing the heating load.

#### 3.4.4. Effect of building height on the total heating/cooling load

As analyzed above, the building height has a negative influence on the cooling load, whereas a positive impact on the heating load. In practical, the building thermal performance is generally investigated via the annual energy consumption. However, it should be noted that only based on the “known” specific configurations of the heating/cooling system, the annual energy consumption of the thousand-meter scale megatall buildings can be simulated, which is beyond the scope of this study. Therefore, we define the maximum hourly cooling load during the simulation period as the design cooling load, and thereby obtain the total value of the heating and cooling load (referred as total load hereinafter) at different heights, based on which the effect of the building height on the total load can be evaluated.

As shown in Fig. 16, for the rooms with different orientations, the vertical variation trend of the total load with the building height is similar; the total load decreases with the increase of the building height, which allow us to conclude that the decrement of the cooling load with height is larger than the increment of the heating load for the case of Dalian. In other words, the rooms at higher levels are potentially energy-saving in the thousand-meter scale megatall building from the perspective of the total load. Additionally, it is evident that the total loads of the room with one external glass certain wall are lesser than those with two external glass curtain walls. For the rooms with one glass curtain wall, the total load gradient of each room is approximately  $-1.1 \text{ W} \cdot 100 \text{ m}^{-1}$ . For a room with two glass curtain walls, the total load gradient of each room is about  $-2.4 \text{ W} \cdot 100 \text{ m}^{-1}$ .

## 4. Conclusions

Meteorological data used for building energy simulation is commonly obtained from standard meteorological stations close to the ground. It is difficult to accurately predict the vertical heating/cooling load distribution for thousand-meter scale megatall buildings with this conventional method. In our study, a united, cross-scale energy simulation method is developed, the goal is not only to simulate the vertical profile in urban scale region, and thereby to improve the heating/cooling load calculation of a thousand-meter scale megatall building, but also to establish a calculation method for accessing the impacts of vertical parameter variation on the heat exchange through building envelopes. The central distinction between united WRF/TRNSYS method and conventional energy simulation program is the consideration of vertical variation of outdoor atmospheric parameter.

Considering there is no existing documentation of more detailed sources for upper level meteorological data in conventional energy simulation programs, establishing such datasets would consume a lot of time and resources. In this paper, we elaborated a united WRF/TRNSYS method on using upper atmospheric data from mesoscale meteorological model WRF as correction to the surface data to improve the heating/cooling considerations of thousand-meter scale megatall buildings. Compared with conventional energy simulation program, it is probably unsuitable for the atmospheric parameters simulated from one specific year to reflect the long-term statistics rules, which is the limitation of the united WRF/TRNSYS method in our study. However, given the lack of more reliable data, the available data from mesoscale meteorological model should provide an alternative in heating/cooling consideration of megatall buildings at present stage.

Moreover, to illustrate the work procedure of united/TRNSYS method better, heating/cooling loads in the typical months are calculated for a hypothetical thousand-meter scale megatall building model in Dalian site as an example, some conclusions based on the hypothetical building are as follows:

- (1) Through long-term simulation by the mesoscale meteorological model WRF v3.4, we obtained a profile of atmospheric temperature and wind velocity at heights from 0 m to 1000 m at the Dalian site. We found that the atmospheric temperature gradient with height is approximately  $-0.57 \text{ }^{\circ}\text{C}/100 \text{ m}$ , and the wind profile is not simply exponential at heights above the atmospheric boundary layer, found to be approximately 300 m above the ground in this study.
- (2) Using the corrected database of TRNSYS 16, the heating/cooling loads for the building model were calculated. The cooling load decreases with the gradient of  $-2.0$  to  $-2.5 \text{ W} \cdot \text{m}^{-2} \cdot 100 \text{ m}^{-1}$ , and the heating load increases with the gradient of  $+1.2$  to  $+2.5 \text{ W} \cdot \text{m}^{-2} \cdot 100 \text{ m}^{-1}$  under the design conditions.
- (3) To discuss the heating/cooling load variation with height quantitatively, the correction factor for height was defined and analyzed. The results show that the cooling and heating load correction factors range from  $-25\%$  to  $-35\%$ , and  $+8\%$  to  $+15\%$ , respectively, for rooms at heights up to 1000 m.

Through the analysis mentioned above, it is found that the vertical variation of the atmospheric temperature and wind velocity has great impact on the heating/cooling load of a megatall building, a fact that should not be overlooked. The united across-scale method, like the WRF/TRNSYS method proposed by this study, is useful for the prediction of the heating/cooling loads of a megatall building. Actually, to simplify the estimation, the vertical variations of other atmospheric parameter, such as the solar radiation and atmospheric pressure, were not considered quantitatively in the united WRF/TRNSYS method at present stage. The effect of these atmospheric parameters on the heating/cooling load, together with the annual energy consumption, will be considered in the further research.

## Acknowledgment

The work presented in this paper was supported by research funding from the China State Construction Engineering Corporation (Project No. CSCEC-2010-Z-01). The authors would like to thank Prof. Shiguang Miao for the help providing meteorological data on this study.

## References

- [1] D. Safarik, A. Wood, M. Carver, M. Gerometta, An all-time record 97 buildings of 200 m or higher completed in 2014, CTBUH J. (2015) 40–47.

- [2] A. Wood, T. Johnson, G.Q. Li, Multi-Disciplinary Paper on Tall Buildings and Sustainable Cities, Council on Tall buildings and Urban Habitat, Shanghai, 2012.
- [3] ASHRAE. ASHRAE Handbook of Fundamentals, American Society of Heating, Refrigerating and Air-Conditioning Engineering Inc, Georgia, USA, 1993.
- [4] C.H. Liu, D.Y.C. Leung, A.C.S. Man, P.W. Chan, Computational fluid dynamics simulation of the wind flow over an airport terminal building, *J. Zhejiang Univ. A* 11 (2010) 389–401, <http://dx.doi.org/10.1631/jzus.A0900449>.
- [5] C. Draxl, A.N. Hahmann, A. Peña, G. Giebel, Evaluating winds and vertical wind shear from Weather Research and Forecasting model forecasts using seven planetary boundary layer schemes, *Wind Energy* 17 (2014) 39–55, <http://dx.doi.org/10.1002/we.1555>.
- [6] C. Mattar, D. Borvarán, Offshore wind power simulation by using WRF in the central coast of Chile, *Renew. Energy* 94 (2016) 22–31, <http://dx.doi.org/10.1016/j.renene.2016.03.005>.
- [7] Y. Sakakubara, K. Nakagawa, Vertical temperature profiles with light breezes at night in urban and rural area of Obuse, Nahano. *J. Geophys.* 120 (2011) 392–402.
- [8] P.A. Irwin, Wind engineering challenges of the new generation of super-tall buildings, *J. Wind Eng. Ind. Aerodyn.* 97 (2009) 328–334, <http://dx.doi.org/10.1016/j.jweia.2009.05.001>.
- [9] T.L. Otte, A. Lacser, S. Dupont, J.K.S. Ching, Implementation of an urban canopy parameterization in a mesoscale meteorological model, *J. Appl. Meteorol.* 43 (2004) 1648–1665, <http://dx.doi.org/10.1175/JAM2164.1>.
- [10] H. Taha, Urban surface modification as a potential ozone air-quality improvement strategy in California: a mesoscale modelling study, *Bound.-Lay. Meteorol.* 127 (2008) 219–239, <http://dx.doi.org/10.1007/s10546-007-9259-5>.
- [11] M.J. Best, Representing urban areas within operational numerical weather prediction models, *Bound.-Lay. Meteorol.* 114 (2005) 91–109, <http://dx.doi.org/10.1007/s10546-004-4834-5>.
- [12] A. Lemonsu, V. Masson, Simulation of a summer urban breeze over Paris, *Bound.-Lay. Meteorol.* 104 (2002) 463–490, <http://dx.doi.org/10.1023/A:1016509614936>.
- [13] K.W. Oleson, G.B. Bonan, J. Feddema, M. Vertenstein, C.S.B. Grimmond, An urban parameterization for a global climate model. Part I: Formulation and evaluation for two cities, *J. Appl. Meteorol. Climatol.* 47 (2008) 1038–1060, <http://dx.doi.org/10.1175/2007JAMC1597.1>.
- [14] K.H. Kwak, J.J. Baik, Y.H. Ryu, S.H. Lee, Urban air quality simulation in a high-rise building area using a CFD model coupled with mesoscale meteorological and chemistry-transport models, *Atmos. Environ.* 100 (2015) 167–177, <http://dx.doi.org/10.1016/j.atmosenv.2014.10.059>.
- [15] Y. Tominaga, A. Mochida, T. Okaze, T. Sato, M. Nemoto, H. Motoyoshi, S. Nakai, T. Tsutsumi, M. Otsuki, T. Uamatsu, H. Yoshino, Development of a system for predicting snow distribution in built-up environments: combining a mesoscale meteorological model and a CFD model, *J. Wind Eng. Ind. Aerodyn.* 99 (2011) 460–468, <http://dx.doi.org/10.1016/j.jweia.2010.12.004>.
- [16] Stensrud, J. David, Parameterization Schemes: Keys to Understanding Numerical Weather Prediction Models, Cambridge University Press, London, 2007.
- [17] R. Shrivastava, S.K. Dash, R.B. Oza, M.N. Hegde, Evaluation of parameterization schemes in the Weather Research and Forecasting (WRF) model: a case study for the Kaiga nuclear power plant site, *Ann. Nucl. Energy* 75 (2015) 693–702, <http://dx.doi.org/10.1016/j.anucene.2014.09.016>.
- [18] R. Borge, V. Alexandrov, J. José del Vas, J. Lumbreras, E. Rodríguez, A comprehensive sensitivity analysis of the WRF model for air quality applications over the Iberian Peninsula, *Atmos. Environ.* 42 (2008) 8560–8574, <http://dx.doi.org/10.1016/j.atmosenv.2008.08.032>.
- [19] D. Carvalho, A. Rocha, M. Gómez-Gesteira, C. Silva Santos, Sensitivity of the WRF model wind simulation and wind energy production estimates to planetary boundary layer parameterizations for onshore and offshore areas in the Iberian Peninsula, *Appl. Energy* 135 (2014) 234–246, <http://dx.doi.org/10.1016/j.apenergy.2014.08.082>.
- [20] W.C. Skamarock, J.B. Klemp, J. Dudhia, D.O. Gill, D.M. Barker, M.G. Duda, X.-Y. Huang, W. Wang, J.G. Powers, A Description of the Advanced Research WRF Version 3, *Tech. Rep.* (2008) 113, <http://dx.doi.org/10.5065/D6DZ069T>.
- [21] J. Xing, P. Ren, J. Ling, Analysis of energy efficiency retrofit scheme for hotel buildings using eQuest software: a case study from Tianjin, China, *Energy Build.* 87 (2015) 14–24, <http://dx.doi.org/10.1016/j.enbuild.2014.10.045>.
- [22] P. Cui, H. Yang, J.D. Spitler, Z. Fang, Simulation of hybrid ground-coupled heat pump with domestic hot water heating systems using HVACSIM+, *Energy Build.* 40 (2008) 1731–1736, <http://dx.doi.org/10.1016/j.enbuild.2008.03.001>.
- [23] E.F. Sowell, P. Haves, Efficient solution strategies for building energy system simulation, *Energy Build.* 33 (2001) 309–317, [http://dx.doi.org/10.1016/S0378-7788\(00\)00113-4](http://dx.doi.org/10.1016/S0378-7788(00)00113-4).
- [24] J.A. Dirks, W.J. Gorissen, J.H. Hathaway, D.C. Skorski, M.J. Scott, T.C. Pulsipher, M. Huang, Y. Liu, J.S. Rice, Impacts of climate change on energy consumption and peak demand in buildings: a detailed regional approach, *Energy* 79 (2015) 20–32, <http://dx.doi.org/10.1016/j.energy.2014.08.081>.
- [25] J. Hu, J. Wu, Analysis on the influence of building envelope to public buildings energy consumption based on DeST simulation, in: *Procedia Eng.*, 2015, pp. 1620–1627, <http://dx.doi.org/10.1016/j.proeng.2015.09.192>.
- [26] S.N. Al-Saadi, Z. Zhai, A new validated TRNSYS module for simulating latent heat storage walls, *Energy Build.* 109 (2015) 274–290, <http://dx.doi.org/10.1016/j.enbuild.2015.10.013>.
- [27] M. Biencinto, L. González, L. Valenzuela, A quasi-dynamic simulation model for direct steam generation in parabolic troughs using TRNSYS, *Appl. Energy* 161 (2016) 133–142, <http://dx.doi.org/10.1016/j.apenergy.2015.10.001>.
- [28] F. Chen, J. Dudhia, Coupling an advanced land surface-hydrology model with the Penn State-NCAR MM5 modeling system. Part I: Model implementation and sensitivity, *Mon. Weather Rev.* 129 (2001) 569–585, [http://dx.doi.org/10.1175/1520-0493\(2001\)129<0569:CAALSH>2.0.CO;2](http://dx.doi.org/10.1175/1520-0493(2001)129<0569:CAALSH>2.0.CO;2).
- [29] S.-Y. Hong, Y. Noh, J. Dudhia, A new vertical diffusion package with an explicit treatment of entrainment processes, *Mon. Weather Rev.* 134 (2006) 2318–2341, <http://dx.doi.org/10.1175/MWR3199.1>.
- [30] E.J. Mlawer, S.J. Taubman, P.D. Brown, M.J. Iacono, S.A. Clough, Radiative transfer for inhomogeneous atmospheres: RRTM, a validated correlated-k model for the longwave, *J. Geophys. Res.* 102 (1997) 16663, <http://dx.doi.org/10.1029/97JD00237>.
- [31] J. Zhou, L. Bao, P. Qian, Study on structural efficiency of super-tall buildings, *Int. J. High-Rise Build.* 3 (2014) 185–190.
- [32] M.A. Mooneghi, R. Kargarmoakhar, Aerodynamic mitigation and shape optimization of buildings: review, *J. Build. Eng.* (2016), <http://dx.doi.org/10.1016/j.jobe.2016.01.009>.
- [33] R. Geiger, The Climate Near the Ground, Harvard University Press, Cambridge, USA, 1973.
- [34] B. Givoni, Climate Considerations in Building and Urban Design, John Wiley and Sons, New York, 1998.
- [35] T.R. Oke, Technical Note No. 134 – Review of Urban Climatology 1968–1973, World Meteorological Association, Geneva, 1974.
- [36] China Meteorological Administration, Qinghua University, Special Datasets of Thermal Environment Analysis for Buildings in China, China Construction Press, Beijing, 2005 (in Chinese).